International Journal of Engineering In Advanced Research Science and Technology ISSN: 2278-2566

December 2016 VOLUME -2 ISSUE-4

Page: 7923-233

SMES/BATTERY ENERGY STORAGE SYSTEM FORELECTRIC BUSES

1. KAVYA A, 2. MD. AIJAZ

PG Scholar, Dept o EEE, Kodada Institute of Technology & Science for Women, Kodada.
 Guide, Dept of EEE, Kodada Institute of Technology & Science for Women, Kodada

ABSTRACT:

The energy balancing problem is the main challenge for the effective application of micro combined heat and power (m-CHP) in a residential context. Due to its high energy density and relative robustness, the lead-acid battery is widely used for power demand management to compensate the mismatch between the m-CHP electrical output and domestic demand. However, batteries are not suited to respond effectively to high frequency power fluctuations, but when coupled to the m-CHP, they experience frequent short-term charge/discharge cycles and abrupt power changes, which significantly decreases their life-time. This paper addresses this problem by hybridising the lead-acid battery storage with superconduct-ing magnetic energy storage (SMES) to form a hybrid energy storage system (HESS) that is coordinated by a novel sizing based droop control method. The control method for the first time considers both the capacity sizing of the HESS technologies and the droop control method of the battery and the SMES. A hardware in the loop test circuit is developed coupling with the real time digital simulator (RTDS) to ver-ify the performance of the HESS with the new control algorithm. The experimental results show that con-trol method is able to exploit the different characteristics of the SMES and the battery to meet the mismatch of m-CHP power generation and domestic demand. In addition, the lifetime analysis is imple-mented in this paper to quantify the battery lifetime extension in the HESS, which further proves the validity of the proposed control strategy. The electricity generated from the m-CHP is fully used in this system (shown by a, b and c).

be met. The HESS works as a kind of power transitional device shifting the power among the m-CHP, the load and the grid (shown by b, d and f), which means the energy storage system will undergo many reverse charge or discharge process. The reverse currents are of great detrimental to the battery lifetime, where the I_{bat conV} is the battery converter current, I_{m bat} is the bat-tery discharge current limit given by manufacturers and the 2 means two cell banks in parallel. It should be figured out that the two parallel where the I_{bat conV} is the battery converter current, I_{m bat} is the bat-tery discharge current limit given by manufacturers and the 2 means two cell banks in parallel. It should be figured out that the

The m-CHP, the HESS and the grid are all able to support the load demand (shown by a, d and e), hence load demand can always

two parallel. In the residential m-CHP system as shown in Fig. 1, for a given load profile and CHP contributions, optimal sizing studies of the HESS should be done to meet both the system energy and power demand. In the proposed SMES/battery HESS, the SMES is sensitive to the short-term high-frequency power fluctuations whereas the battery is designed to deal with the large energy demand. The SMES has large power capacity but cannot store much energy, so the battery is expected as an energy buffer to the SMES. The capacity of the HESS needs to meet both the power and energy require-ment to fulfil the power/energy management functions. The hybrid sizing study method which is able to effectively take advantage of different characteristics of ESSs to determine the capacities of the SMES and the battery has been developed in [34], and therefore, is used in this study. It is out of this paper's scope to introduce the precious sizing method in detail but the detailed size parameters of the battery and SMES are given in Appendix, Tables A1 and

1. Introduction

The major challenges in power systems are driven by environmental concerns, namely facilitating penetration of renewable energy and improving the efficiency of fossil fuel based generation [1]. In the long term, the transition to a fully renewable energy mix will solve mounting environmental problems from intensive com-Compared with the conventional single technology energy stor-age system, the control algorithm for a HESS is more complicated because of the requirement to effectively combine the harmonious operation of two storage technologies such that they complement each other. The co-ordinated HESS control must achieve real time system optimisation

bustion of fossil fuels [1–3]. In the short term however, developing a more efficient energy system using existing energy conversion infrastructure is considered a vital transitionary pathway to a low carbon future by both policy makers and academic experts [3–5]. One of the most promising technologies in achieving this transition is micro-combined heat and power systems [5–8].

M-CHP systems which broadly range from 1 kW and 15 kW in capacity [5,7–9], are able to take advantage of the waste heat from the heat engine for building heating and hot water requirements. By harnessing the wasted thermal energy, the overall efficiency of m-CHP can be raised to over 80%, up from approximately 20%

for an equivalent rated generator [4,6,10,11] thus dramatically increasing primary energy savings.

The buildings and housing sector accounts for a significant proportion of the primary energy demand: about 60% in the EU [12], over 50% in the UK [13] and averaging approximately 40% in most developed countries [14]. Many previous works have investigated the benefits of using m-CHP in a domestic setting. Maghanki et al. conclude from an energy perspective that the m-CHP is able to meet most of the domestic thermal energy demand, achieving over 20% energy saving index [6]. The m-CHP system is predicted in [9] to meet about 25–46% of annual energy demand of a typical British household, together with achieving over 40% reduction in the peak electrical load in the winter days.

However, energy balancing is one of the major challenges for the effective application of m-CHP in a residential context. Several factors combine together to exacerbate this problem, namely: (a). load demands are highly fluctuating, often with random seasonal components, which may cause intermittent bi-directional flows of electricity [9,15]; (b). tariff design impacts the operation of m-CHP, which makes the power balancing more complicated [1,3], (c). the thermal energy and electric power demands often do not coincide with each other [1,15]. To solve these problems, localised energy storage systems have therefore often been proposed as a complementary technology to m-CHP [2,3,16]. M-CHP systems with high heat to power ratio are more suitable for domestic applications where the power demand is continuously much lower than the heating demand [1]. In such systems the CHP is dispatched to follow the heating load, which gives a stronger indication for electrical energy storage than thermal storage. This paper therefore mainly focuses on the electric storage system in a residential m-CHP system.

Battery energy storage systems have high efficiency, large energy density, high levels of robustness and the inherent ability to load shift and are therefore widely used in many power applications (e.g., electric vehicles and distributed generation). Due to the technical maturity and relative low cost, the lead-acid battery is an ideal solution for domestic demand response management [17,18]. However, the lead-acid battery has a very low power density resulting in a slower response speed to fluctuations in demand [19]. The highly variable output and demand mismatch of a residential m-CHP leads to more discharge and charge cycles and also accelerates the battery's degradation process, resulting in shorter battery service life and increased battery replacement costs. To address these problems, the inclusion of another complementary storage, to form a hybridized energy storage system (HESS) has therefore been the focus of much recent research. For example battery storage hybridised with supercapacitors have been widely investigated in many power applications, with the benefits shown to be of improved system response speed and the extension of battery lifetimes. Xiong et al. proposed a near-optimal power management strategy for battery and supercapacitor hybrid system. Both battery durability and longevity performance have been considered in this method and the results shows a good performance for the EVs against uncertain diving cycles [20]. Compared with supercapacitors, superconducting magnetic energy storage has higher power density, lower self-discharge rate, and higher peak current handling capabilities [21-23]. Despite these advantages fewer studies focus on the SMES/battery HESS because of the present high costs of SMES. However with the continuous development of superconductive material, some recent studies show positive cost-benefit analysis of SMES [24,25]. One of the novel contributions of this paper therefore, is to study the composite impact of m-CHP, variable tariffs and load demands on the battery in a domestic setting. Then, a SMES/battery HESS is designed for a domestic context that protects the battery from unnecessary charge/discharge cycles and hence, extends the battery lifetime.

Compared with the conventional single technology energy storage system, the control algorithm for a HESS is more complicated because of the requirement to effectively combine the harmonious operation of two storage technologies such that they complement each other. The co-ordinated HESS control must achieve real time system optimisation which also harnesses advantages of both technologies whilst eliminating their disadvantages. Many power control algorithms for HESS are reported in the literature. Fuzzy control, which can realize power management in nonlinear systems without precise system modeling has been proven highly suitable for coordination of multiple energy sources. Ise et al. [21] propose a fuzzy control based method in railway power systems, achieving effective power sharing between the battery and the SMES. Similarly, fuzzy control has been used for power management of the HESS in electric vehicles [26-28] and wind applications [29] with the benefits of protecting the battery and improving system efficiency. However, some specific constraints and fuzzy regions used in this control are selected empirically. which sometimes may lead to sub-optimal design choices. Li et al. [30] and Song et al. [31] proposed the conceptually simple power grading control that classifies the power requirements manually and distributes the power demands to the different energy storage systems based on their classification. Obviously, accuracy of this controller is highly dependent on the specific implementation. The filter based power control method which uses the inherent filtration characteristic of the SMES and supercapacitors to allocate low frequency charge cycling to the battery has been applied in micro-grid applications [32], EVs [33] and renewable generation [34]. The main problem with this technique is that the optimal cut-off frequency of the filter is very difficult to determine. Model predictive control has been show to effectively reduce battery peak currents in a HESS [35], but at the cost of poor efficiency of the short-term energy storage system. Allègre et al. [36] introduce a real-time data driven control of the supercapacitor/battery HESS achieving a high utilization factor of the supercapacitor by delaying battery activation until after the supercapacitor reaches its voltage limitation. The drawback of this approach is that the battery may be damaged when the supercapacitor is fully discharged.

Droop control, which is able to take advantage of various kinds of power sources to match different load demands, has been proven to have a high efficacy in a decentralized DC grid [37], renewable sources [38,39], EVs [40] and AC grid [41]. It achieves optimal allocation of multiple energy sources to various demands by setting appropriate droop coefficients for different converters [39,40,42]. The main challenge for droop control is to select the optimal droop coefficients for different energy

Appropriate sizing is another challenge for HESS design. Despite the fact that clearly the capacities of each energy storage in the HESS have great impact on the power sharing control, few studies have integrated a capacity sizing method together with the control method. Therefore, the main contribution of this paper is a novel sizing-study-based droop control for the power sharing between the SMES and the battery. The new method integrates the sizing study into the droop controller by using the sizing results of the HESS to determine the droop factors. In this way, not only the capacities of the ESSs have been taken into account in the control algorithm but also the appropriate droop coefficients have been generated.

The extension of the battery service time is one of the key advantages of the hybrid energy storage design. In order to verify the proposed SMES/battery hybrid design, and its control method, the battery lifetime analysis has been conducted to quantify the battery lifetime extension in the HESS. A hardware-in-the-loop (HIL) testing system is developed and coupled with a real time

digital simulator (RTDS), which is used to demonstrate the hybrid energy storage in the residential m-CHP system.

The paper is organized as follows. Section 2 gives the overall system configuration and an overall power management strategy. The novel control method is introduced in Section 3 including the HESS sizing study, the droop factor modification and detailed control methods for the converters. Section 4 illustrates the HIL real-time test platform in details. After that, the results are analysed and discussed. The quantified analysis of battery lifetime extension is implemented by introducing a battery lifetime model in Section 5. The cost analysis of the proposed hybrid design is introduced in Section 6. Finally, the conclusions are presented in Section 7.

2. System description

2.1. System configuration and modeling

Fig. 1 shows the configuration of the proposed domestic power system including the m-CHP, the battery, the SMES, power converters, the grid and the demotic load. The battery and the SMES are controlled using two bidirectional DC/DC converters and then interfaced with the AC bus by a DC/AC converter. All the power converters are modeled using the small-time-step model in the RSCAD software [43], but the novel control algorithm is implemented in the external hardware, which is introduced in detail in Section 4. The SMES are modeled as an equivalent large inductance using the method described in [34,44]. The parameters of the battery and the SMES subsystem are given in detail in Appendix, Tables A1 and A2. In the UK, the m-CHP rates at up to 16 A per phase and therefore prime mover capacities of up to about 2.7 kW are of interest [9]. As introduced in Section 1, this study mainly focuses on electric energy part therefore, the m-CHP is built using the method described in [45] but, the heat generation from the CHP is not considered.

2.2. System power flowing design

In order to improve the energy efficiency and achieve coordination control of different devices, an overall power management strategy is needed. Fig. 2 shows the power flow paths in the power management strategy:

- a. In normal condition, the electrical power generated from the m-CHP (P_{CHP}) will support the load demand (P_{load}) , preferentially.
- b. The m-CHP will charge the HESS when $P_{CHP} > P_{load}$ and the battery state of charge $SOC < SOC_{max}$, the up-limit of battery SOC (97%). It should be figure out that, the SMES has low energy density which means it cannot storage much energy and in this study the battery is designed as energy buffer to the SMES. Hence, the battery state of charge is used as charge/discharge criterion of the HESS
- c. The residential power system will export the electricity to the grid when $P_{CHP} > P_{load}$ and SOC P SOC_{max} .
- d. The HESS system will discharge to meet the load demand when P_{CHP} < P_{load} and SOC $\stackrel{\textstyle >}{\sim}$ SOC_{min} (20%).
- e. The residential power system will also buy electrical power in two conditions: 1. $P_{CHP} < P_{load}$ and $SOC \ 6 \ SOC_{min}$ or 2. $P_{CHP} < P_{load}$ and the time-of-use electric tariff is low.
- f. The grid will also charge the battery when the tariff is low and battery SOC 6 SOC_{max}.

The main function of the overall power flow control, in this paper, is to obtain the power export and import requirement of the HESS with the consideration of the varying load profiles, the inconstant CHP power output and the electric tariffs. The six power flow paths also illustrate other key points of the overall power management strategy:

The electricity generated from the m-CHP is fully used in this system (shown by a, b and c).

The m-CHP, the HESS and the grid are all able to support the load demand (shown by a, d and e), hence load demand can always be met.

The HESS works as a kind of power transitional device shifting the power among the m-CHP, the load and the grid (shown by b, d and f), which means the energy storage system will undergo many reverse charge or discharge process. The reverse currents are of great detrimental to the battery lifetime.

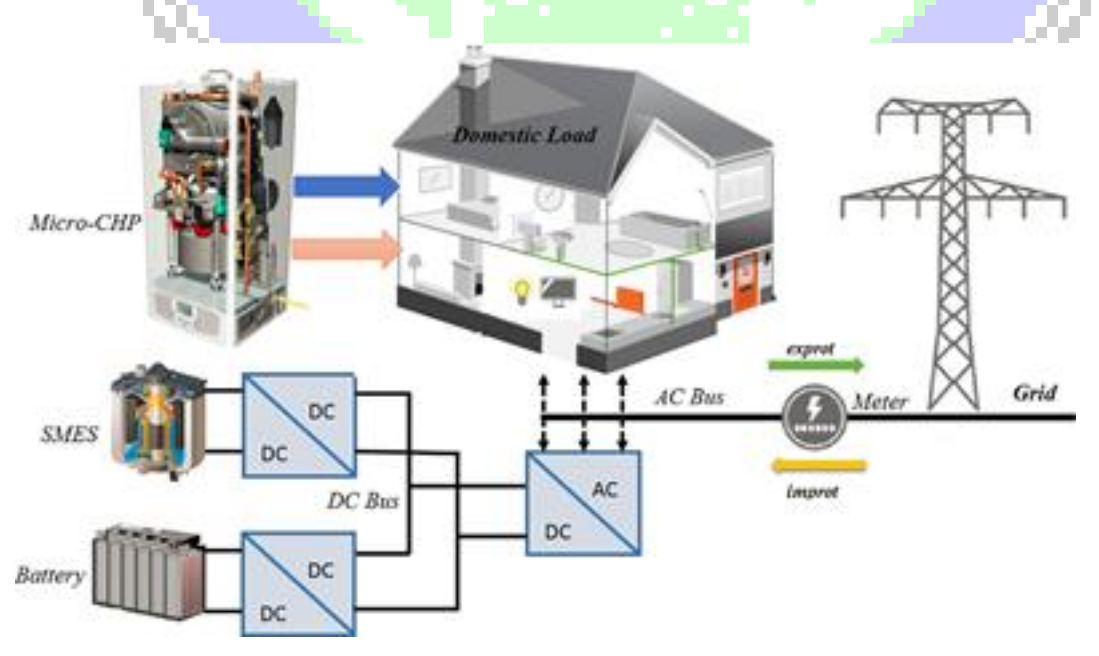


Fig. 1. The residential m-CHP system with the SMES/battery HESS.

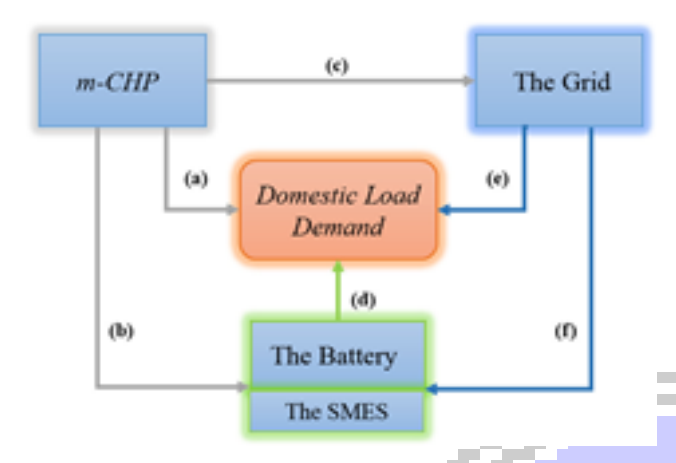


Fig. 2. The power management strategy.

The proposed domestic power system is able to either export or import the electric power according to the time-of-use electric tariffs (shown by c, e and f). It should be noted that in this paper, only high and low tariff states are used as the criterion.

The battery is kept within a safe operating region by setting the up and bottom limits.

3. Novel control of the HESS

3.1. The droop control

The power fluctuations in the AC side are seen by the AC/DC converter resulting in the DC bus voltage variations. In order to maintain the DC bus voltage in the desired range, the ESSs need to be controlled to charge or discharge. For the proposed hybrid energy storage system, the control algorithm should be able to share the power demand between the SMES and the battery according to their different characterizes. The bidirectional droop control has already been successfully implemented in many applications achieving decentralized control of different energy storage systems [11,38,40,41]. The DC/DC converter controlled by the bidirectional droop characteristic is able to generate different converter reference signals to charge/discharge the different energy storage devices at different rates. Fig. 3 shows the working principle of the bidirectional droop control. Based on the DC bus voltage, the ESSs inject or absorb currents at the level controlled in the following three cases:

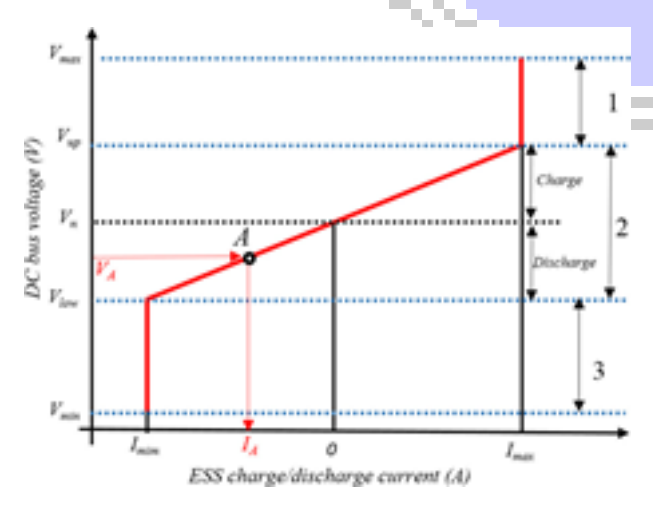


Fig. 3. The bidirectional droop control for energy storage.

- 1. When $V_{bus} P V_{up}$ (where the V_{bus} is DC bus voltage and the V_{up} is the upper voltage limit of the energy storage device), the ESSs will absorb the surplus energy in the maximal current I_{max} .
- 2. When V_{low} 6 V_{bus} 6 V_{up} , the ESSs will charge or discharge in the current I which may be obtained by the Eq (1).

I ¼ ðV_{bus}

where the V_r is the reference voltage and the f is the droop factor of a certain energy storage system. For example, given a DC bus verify age measurement as V_A , then based on the droop control and Eq (1), the ESS is controlled to discharge at the current of I_A and I_A V_A V_{bus}

- 3. When V_{bus} 6 V_{low} the ESS dischar* (q.*) at maximum discharge current I_{min} .
- f. The real-time DC bus voltage is derived from measurement. The maximal and minimal voltages (V_{max} and V_{min}) of the ESS are selected to protect the ESS from over charge/discharge. The reference voltage is predefined as the system normal voltage. The droop control method is able to prioritize the operation of the SMES over the battery by selecting a lower SMES sensitive voltage. One of the advantages of the droop control is that the different ESSs are able to compensate the voltage deviation at their own rate of current by setting the different droop factors. V_{up} and V_{low} are critical factors that determine the droop coefficient and they are selected based on the system sizing study.

3.2. System sizing study

In the residential m-CHP system as shown in Fig. 1, for a given load profile and CHP contributions, optimal sizing studies of the HESS should be done to meet both the system energy and power demand. In the proposed SMES/battery HESS, the SMES is sensitive to the short-term high-frequency power fluctuations whereas the battery is designed to deal with the large energy demand. The SMES has large power capacity but cannot store much energy, so the battery is expected as an energy buffer to the SMES. The capacity of the HESS needs to meet both the power and energy requirement to fulfil the power/energy management functions. The hybrid sizing study method which is able to effectively take advantage of different characteristics of ESSs to determine the capacities of the SMES and the battery has been developed in [34], and therefore, is used in this study. It is out of this paper's scope to introduce the precious sizing method in detail but the detailed size parameters of the battery and SMES are given in Appendix, Tables A1 and A2, respectively.

3.3. Droop factor modification

As introduced at the very beginning, the droop control is capable of combining multiple ESSs according to their own features by selecting different droop coefficients. However, to the authors best knowledge, there is no published work describe how to determine the different droop coefficients for different ESSs. This paper proposes a new method which takes the size and various constraints of the ESSs into account, to give the reasonable ranges of the droop factors for both the battery and the SMES.

3.3.1. The battery droop factor

Normally, there is an optimal discharge range for the batteries. The over-range discharge current will accelerate the degradation process of batteries. The decrease of the battery peak current is one of the benefits of using the HESS. The battery manufacturers often give the discharge current limit beyond which the battery terminal will drop dramatically. In addition, as shown in the Appendix Table A1, the battery is sized in the structure of two cell

banks in parallel. Therefore, the first operation constraint can be obtained:

$I_{bat. conV}$ 6 2

where the $I_{\text{bat. conv}}$ is the battery converter current, I_{m} bat is the battery discharge current limit given by manufacturers and the 2 means two cell banks in parallel. It should be figured out that the two parallel banks cannot always perform in the same way and the unbalances between the battery banks have a potential impact on the control. To solve this problem, the error allowance bands are added to the battery parameters used in the control algorithm. Also, in the proposed study, the battery model is established in the RTDS which is a kind of ideal simulation environment rather that the real-life environment. Hence, the chance of the battery unbalance problem is much less.

The battery provides large energy to compensate the unbalanced power in the residential system. Therefore, the energy requirement should be always met, which generates the following constraint:

$$I_{\text{bat, conV}} = V_{\text{bat}}$$

where P_{mis} it is power in the system sizing process, V_{bat} is the battery normal voltage and t is the simulation duration.

Based on the Eq. (1), the \mathbf{g}_{bat} defined as the battery converter voltage fluctuation allowance is used to link the battery converter current with the drop factor:

$$f_{bat} \% \frac{I_{bat, conV}}{\delta V_{bus}} \% \frac{I_{bat, conV}}{\delta V_{bus}}$$
 ð4Þ

The g_{bat} as can be deduced from Fig. 3:

The up voltage limit of the battery $V_{up,\,batt}$ can be obtained by giving the battery capacity E_{batt} and battery expected longest discharge time T_{bat} :

$$V_{\mathrm{up,\,batt}}$$
 ¼ $\frac{E_{\mathrm{batt}}}{T_{\mathrm{bat} \ \mathrm{m} \ \mathrm{bat}}}$ 06Þ

From Eqs. (2)–(6), the f_{bat} can be deduced in the range shown in Eq. (7):

(7): I
$$R_{0}^{t}P_{mis}\delta t P dt$$
 $G f$

The E_{batt} is sized as 240 Å h, and the expected longest discharge time at the maximal current limit T_{bat} is set as one hour, hence the f_{bat} is larged from 0.32 to 0.72. To protect the battery from the high-peak current, the value of 0.32 is selected as the droop factor of the battery subsystem.

V_{bat}

2

3.3.2. The SMES droop factor

Firstly, works as a kind of short-term energy storage system the SMES has high power capacity and should be able to deal with most of the immediate power surplus or deficiency. Therefore, the first constraint that the SMES power should not be less than maximum mismatch ($P_{mis, max}$). If the SMES converter current is $I_{S, conV}$ and the normal SMES converter voltage is V_{S} , then Eq. (8) can be obtained:

$$I_{S. \, conV} \, \, m{P} \, \frac{P_{mis, \, max}}{V_S} \,$$
 ő8Þ

In addition, the DC current flowing through the SMES coil is limited by the critical current (I_c) beyond which the superconductor will

quench. Considering the largest duty ratio (D = 1) of the SMES converter, the converter current equal to the SMES current. Hence, the constraint shown in Eq. (9), can be obtained.

The g_{SMES} is defined as the SMES converter voltage fluctuation allowance, based on the Eq. (1), the droop factor of the SMES subsystem can be written as:

$$f_{SMES} \frac{1}{\sqrt[3]{dV_{bus}}} = \frac{1}{\sqrt[3]{dV_{bus}}} = \frac{1}{\sqrt[3]{dV_{bus}}}$$
 510b

Similar ψ_0 the battery, the g_{bat} as can be deduced by Eqs. (11) and

$$g_{\text{SMES}}^{Q_{\text{SMES}}} \frac{2\delta V_{\text{up. SMES}}}{V_{\text{S}}}$$
 $\delta 11$

$$V_{\text{up. SMES}} \frac{1}{4} \frac{E_{\text{SMES}}}{T_{\text{SMES}} + m. \text{SMES}}$$
 012b

where T_{SMES} refers to the longest discharge time at 80% I_c.
According to Eqs. (8)–(12), the f_{SMES} is ranged as:

Mimited by the cooling system, the SMES critical current I_c is selected as 270 A. Based on the other parameters given I_c is selected as 270 A. Based on the other parameters given I_c is than 8.7 Mes. The cycle life of the SMES is almost unlimited which means the SMES could charge and discharge in a high frequency without any degradation. I the HESS, the SMES are expected charge and discharge as deep as possible and therefore the largest droop factor 0.87 is selected in this study.

3.4. The DC/DC converters

A bidirectional synchronous-buck DC/DC converter is used as the battery controller in this study. The hysteresis control presented by [39] has good tracking capability and high-robust, hence is applied in this study to control the battery converter. Li et al. in [39,42] introduced a similar asymmetric full bridge DC/DC converter to control the charge and discharge current flowing through the SMES coil. This H bridge design is able to take advantage of the fast response of the droop control and the charge/discharge current rate can be directly by the droop factors. The SMES DC/DC converter is built according to the previous work described in [39].

4. Real-time verification

4.1. Laboratory test system configuration

A hardware in the loop test circuit is developed working together with the RTDS to verify the proposed control algorithm. As shown in Fig. 4, the residential m-CHP system is built in the RTDS which takes advantage of the real-time simulation capability and system flexibility of the RSCAD. The main novelty of this study is the new control method, so in order to effectively verify the main contribution of this paper, all the control algorithms are written in the external circuit using DSP TMS320F28335. Fig. 4 shows the configuration of the HIL test platform. The main devices include the real time simulator, the analogue interface, the DSP and the digital interface. It should be figure out that, both a digital to analogue card (ODAC card) and an analogue to digital card (GTDI card) are inlayed in the RTDS.

Moreover, as shown in Fig. 4, the signaling process may be illustrated in 5 steps: 1. The parameters that used for the control are

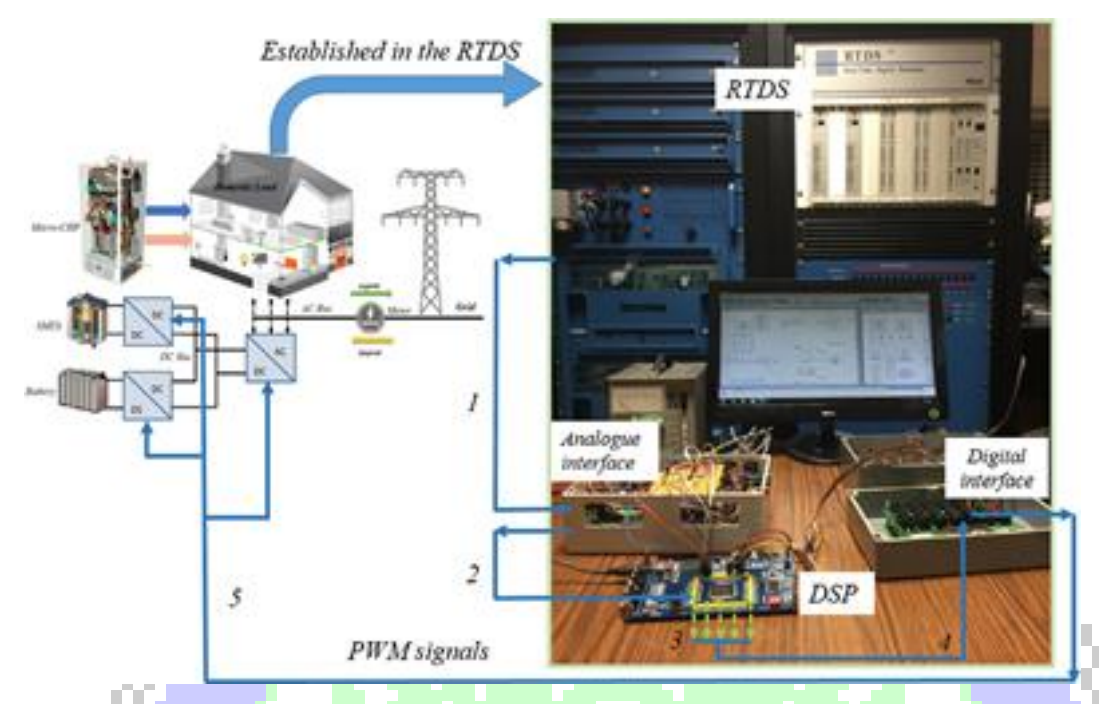


Fig. 4. The hardware in the loop system configuration.

measured by the RTDS and sent to the interface as analogue data; 2. The analogue output signals are captured by the DSP from the analogue interface; 3. DSP generates the PWM control signals based on the measurement using the novel control algorithm; 4. The digital control signals are sent to the digital interface and then 5. The control PWM signals are read by the GTDI card in the RTDS and delivered to the converters. As a result, the converters in the RTDS is controlled by the proposed control algorithm that implemented in the outside DSP circuit. The sampling rate of the digital to analogue card is 50 ls. The switching frequency of the converters is selected as 2.5 kHz in order to increase the resolution the PWM signals. The normal DC bus voltage regarded as reference voltage in this system is 500 V, the initial SMES current is 150 A and the other parameters of the test system can be found in the Appendix, Table A3.

4.2. The experimental results and discussion

Figs. 5 and 6 show the experimental results in two scenarios: the domestic power system with SMES/battery HESS and with battery only system. Using the power flowing control method introduced in Section 2.2, the net power requirement for the energy storage can be obtained. Figs. 5 and 6 show the same power demand with the duration of 40 s (10–50 s) in the two scenarios.

As shown in Fig. 5, in the first 10 s, the power demand is ——500 W and this amount of power surplus will raise the DC bus voltage. However, in order to maintain the DC bus voltage in the desired range, the SMES current rises to 162 A and the battery has a negative current, which means both the SMES and the battery come into action to absorb the excess energy.

Also, in Fig. 5, when the power demand becomes 500 W in the following 10 s, the SMES current encounter with a dramatic decrease from 162 A to 114 A to discharge the stored energy. The battery current changes from negative to positive but compared with the SMES, the battery current climbing speed is much slower. This verify the benefit of the HESS that the SMES is controlled to deal with the immediate power changes while the battery provide long-term energy support to compensate power fluctuations. In

this way, the battery is protected from the abrupt high power changes.

In the third 10 s, there is no surplus or deficient power flowing in the system, but as it can be observed from Fig. 5, the SMES current increases, which means the SMES is charged. In addition, when there is no power demand, the battery current does not come to the zero but stay in a positive value to discharge its energy. The reason for this phenomenon is that the SMES current is lower than the initial current hence the battery delivers its energy to charge the SMES. This situation further proved the HESS control that the battery works as an energy buffer to the SMES and at the same time, is kept from the immediate change of state.

In contrast to the SMES/battery HESS, Fig. 6 shows the system performance of the battery only case. As it can been seen from Fig. 6, the battery current changes immediately with the power demand variations. These abrupt changes of the current will accelerate the battery degradation process hence reducing battery service life. In addition, the DC bus voltage is not as stable as that in the HESS and some cusps can be observed at the power change points. The zooming in figures of the DC bus voltage and the battery current at the power change point (20 s) may be used to explain the cause of the cusps. The battery is modeled as the lead-acid battery which cannot response very quickly to the power demand, hence cause the delay of the charge/discharge current, resulting in the jut of the DC bus voltage.

5. Battery lifetime analysis

5.1. Battery lifetime prediction model

As one of the key advantages of the proposed HESS, the development of the battery service time should be analyzed. Therefore, it is necessary to build a battery lifetime prediction model in this study to evaluate the battery lifetime extension. In order to perform a precisely prediction, various factors such as battery working conditions, the discharge rate, and the capacity fading mechanism, need to be considered [46,47]. Some unpredictable factors may also contribute to the battery degradation process. Moreover, there

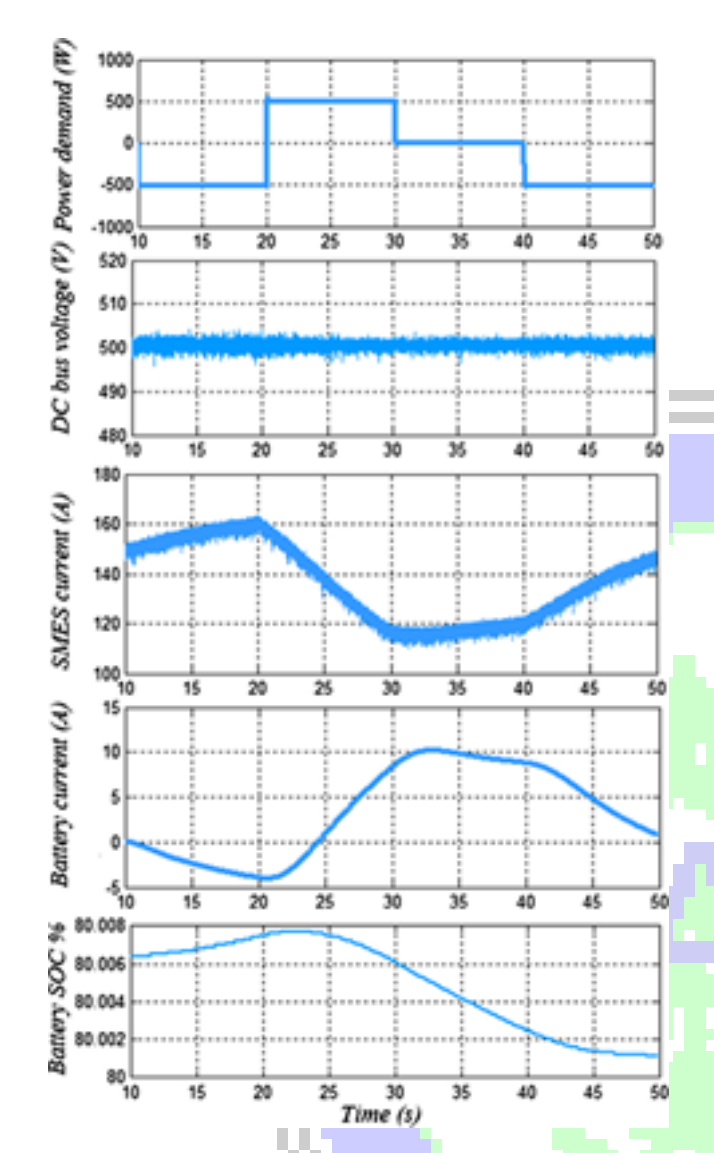


Fig. 5. Experimental results in the SMES and battery HESS.

are many uncontrolled interactions between the different degradation factors which make the battery aging processes extremely non lineal [48,49], hence currently, it is hardly to create a practical battery lifetime model. Whereas, some simplified battery lifetime models which only consider the key influences have been proved accurately enough in some applications. The lifetime model based on the rain-flow cycle counting algorithm have been successfully used in many studies and have been proved very suitable for battery lifetime analysis in a hybrid energy storage system [50–52].

In the proposed hybrid energy storage, the battery lifetime can be improved in two ways: firstly, the SMES deals with most of the short-term power demand, which reduce the battery cycling times; secondly, the battery is protected from high abrupt power changes. The battery degradation model based on a kind of modified rain-flow cycle counting algorithm [34] as shown in Fig. 7, is able to quantify both the depth of discharge (DOD) and discharge rate of each cycle and therefore used in this study.

As shown in Fig. 7, the input data for the algorithm is the battery depth of discharge data during the simulation time T. The rain-flow cycle counting method which was firstly used for metal fatigue estimation [53], is suitable for analyzing the DOD array of the battery. By using this method, the irregular charge and discharge cycles are resolved into sub-cycles and then recomposed into an array of full cycles. Then, three factors, the total cycle num-

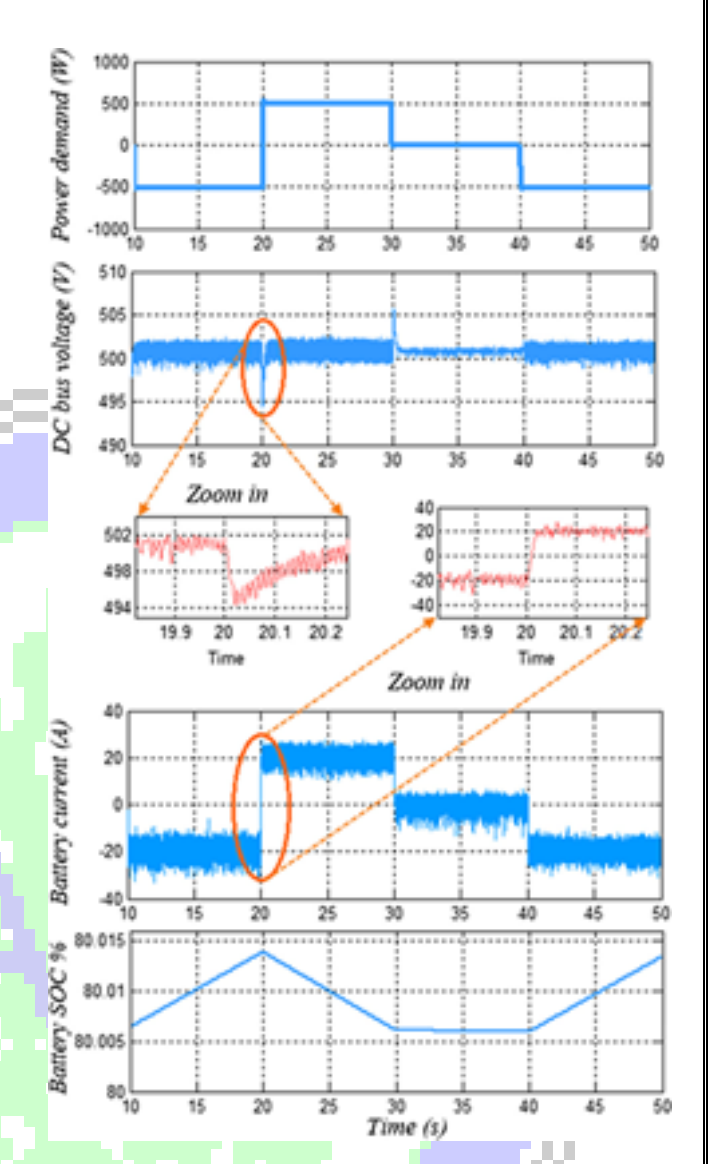


Fig. 6. Experimental results in the battery only system.

ber N, the DOD of each rearranged full cycle and the C-rate of each cycle, can be obtained as shown in Fig. 7. For the lead-acid battery, the capacity degradation is proportional to the depth of battery discharge. Based on the "cycle-to-failure" method described in [34,54], this paper estimates the embryo cycle number C(i) of battery at the DOD(i). Then, as shown in Fig. 7, the impact factor $\mathbf{1}(i)$ of the C-rate (i) can be calculated based on the battery lifetime modeling. The abecedarian cycle number C(i) multiplied by $\mathbf{1}(i)$ will return to the revised cycle number C(i). Then, the effect on battery lifetime of cycle i is d(i), where d(i)=1/Cr(i). Therefore, the total degradation of battery lifetime D can be written as Eq. (14).

With the given simulation duration T, the predicted battery lifetime L_{bat} can be obtained with Eq. (15):

5.2. Battery lifetime extension qualification

and Fig. 9 the battery only system. Comparison of Figs. 8 (a) and 9(a) illustrates that the battery in the HESS experiences

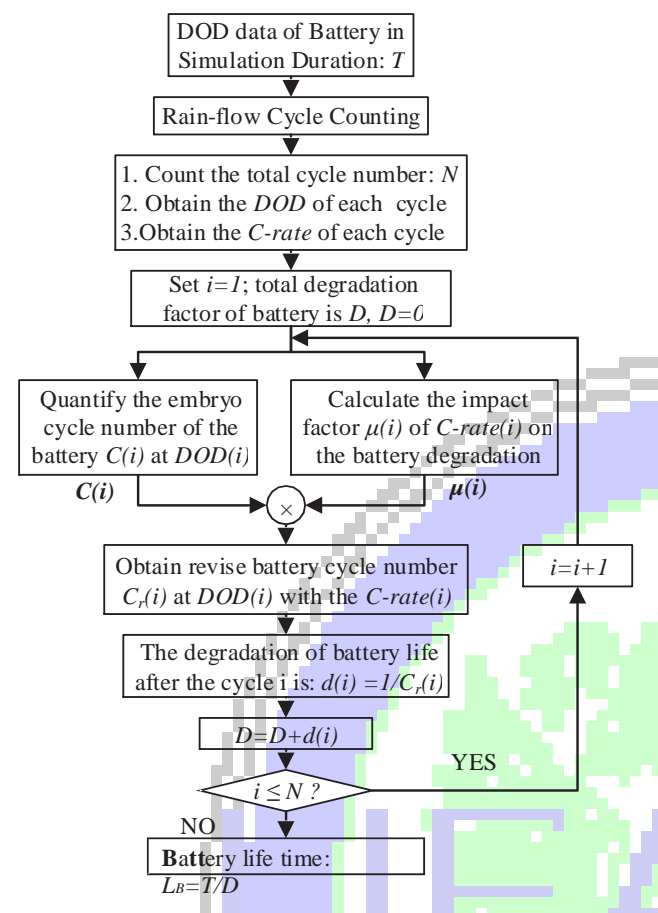


Fig. 7. Battery lifetime prediction algorithm.

significantly fewer high frequency fluctuations and polarity reversals. As a result, the state of charge (SOC) in the HESS (Fig. 8(b)) undergoes less short-term charge and discharge cycles than that in the Battery only system (Fig. 9(b)). The battery lifetime model used in this study will return to a parameter called degradation factor which can be used to describe the relationship of battery DOD and discharge current rate to the battery life-span [34]. The 3-D plots are used to show a visualized tendency of lifetime extension in the HESS: the smaller area of the plotted figure and lower value of degradation factors proved the synergic impact of the reduced cycle numbers and the decreased discharging current resulting from the active hybridization of SMES and batteries.

In the case of the SMES/battery HESS, the predicted battery lifetime is 8.7 years whereas the number of that in the battery only system is only 6.2 years. Hence, the 2.5 years (over 40%) extension of battery service lifetime is achieved.

6. Cost analysis

The superconducting energy storage system is costly because of the material cost and the high investment of the SMES is the main reason that discourages people from using it. However, in the hybrid energy storage scheme, with the integration of the battery the size requirement for both the SMES and battery can be dramatically reduced. Also, compared with the battery only system (BOS), the hybrid design has the advantage that extension of battery lifetime. As the introduced in Section 5, the battery service life is quantitatively improved by 40% from 6.2 years to 8.7 years. Moreover, with the fast development of superconductor manufacturing technology, there are more and more commercial companies

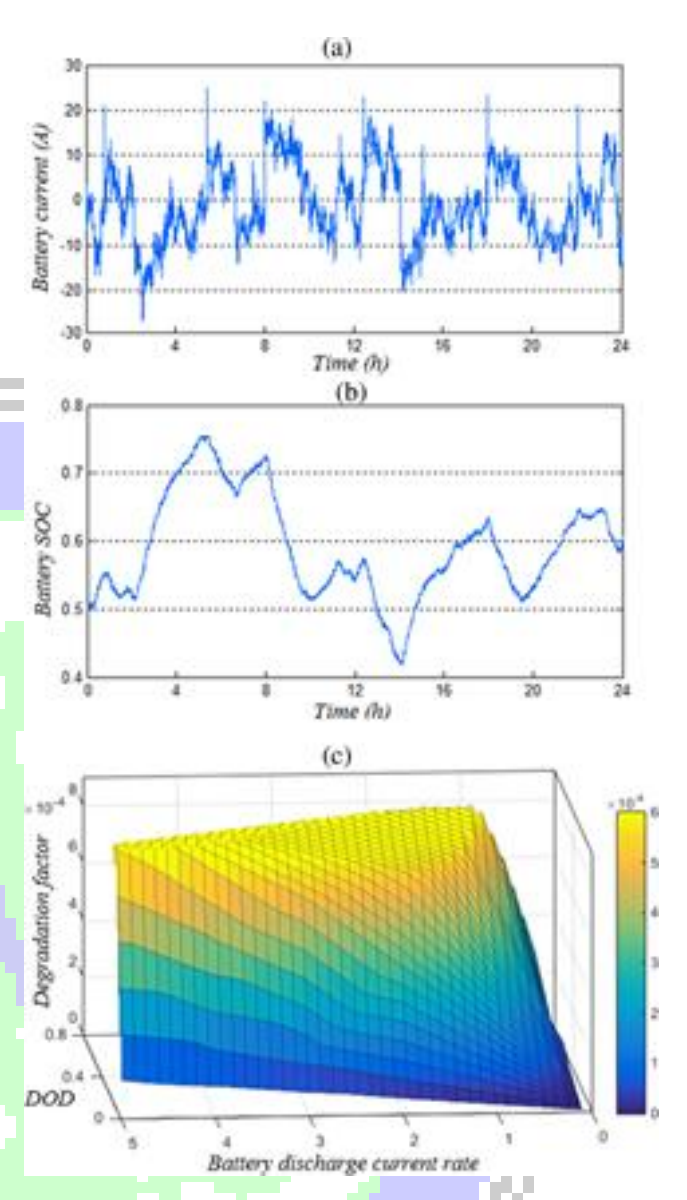


Fig. 8. SMES/battery HESS results (a) battery current, (b) battery SOC, and (c) 3-D plot of battery degradation.

around the world being able to produce the cheap superconducting tape, such as SuNam and Shanghai Superconductor [55,56]. The price of the superconductor is reduced from \$60 per meter in 2012 to \$22 per meter in 2016, which is a significant cost reduction in the last five years. Some published works also make the estimation that in the further, it is achievable to decrease the price of superconductor less than \$10 [57,58]. Therefore, with the continuous development of superconductive material, it could be known for sure that the cost of SMES could be further reduced.

As introduced in Section 3.2 the energy storage devices need to meet both the power and the energy requirement of the residential system. Based on this principle, the SMES is selected as 5.27 kJ and the 4 battery cells (60 A h each) are the need. If only the battery energy storage system used in the same situation, based on the same sizing method, extra 24 battery cells are needed to meet the instantaneous power demand. Based on the SMES design method [59,60] and the up-to-date superconductor price [57] the total cost of the 5.27 kJ SMES is \$44.8 k including the cryocooler. The unit price for the 60 A h lead acid battery is quoted as \$245. The total lifetime of the energy storage project is assumed as

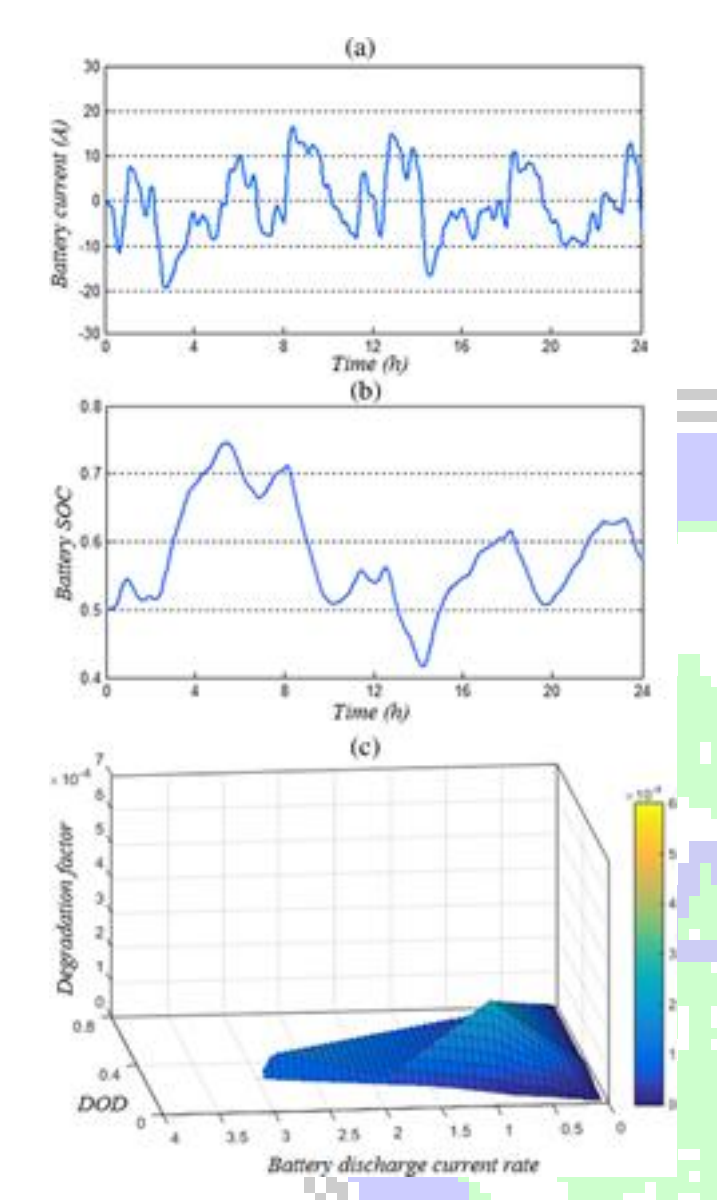


Fig. 9. Battery only system results (a) battery current, (b) battery SOC, and (c) 3-D plot of battery degradation.

35 years. There is almost no lifetime degradation for the SMES system hence the SMES in the hybrid design does not need to be replaced. Based on the lifetime analysis in Section 5, the battery in the hybrid scheme need to be replaced 4 times whereas in the battery only system the number of that is 6. Table 1 illustrates the investments in the proposed two cases.

As shown in Table 1, the total cost of the SMES/battery hybrid system is higher than that of the battery only system by 18.37%. The estimation of Table 1 is based on the price of \$22/m for the superconductor tape. However, as mentioned earlier, with the continuous development of superconductive material, the price

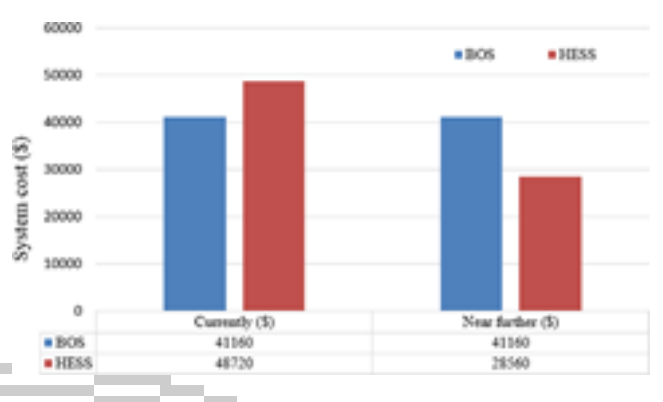


Fig. 10. Comparison of the system costs.

of the superconductor has been decreasing and it is believed that the price will reduce down to at least \$7.2/m in the near future [55,57,58]. Based on the same cost analysis method, the result will change for sure that the hybrid design will be more economical in the near further. As shown in Fig. 10, if the superconductor decreases to \$7.2/m, the system cost of the hybrid energy storage will reduce to \$28,560 which is 30.6% cheaper than the battery only system.

7. Conclusion

This paper investigates the use of a SMES/battery hybrid energy storage system in a domestic power system with m-CHP. A novel HESS control method which advances the previous droop control by introducing the HESS sizing factor into the droop coefficients definition is presented to prioritize the power demand sharing between the SMES and the battery. In order to verify the new control method, the hardware in the loop test circuit is established coupled with the real time simulator. A representative domestic grid connected power system with the m-CHP and the HESS is developed in the software RSCARD and the physical control signals are generated by the DSP in the external circuit. The experimental results show that the proposed control method is able to exploit the different characteristics of the SMES and the battery to meet the unbalance power in the residential system. The battery in the experiment is protected from the continual short-term charge/discharge cycles and abrupt power changes and, as a result, the battery lifetime is improved. Therefore, a quantitative analysis of battery lifetime extension in the HESS has also been done in this study. Based on the proposed domestic power system, the battery lifetime is improved from 6.2 years in the battery only system to 8.7 years in the hybrid energy storage system. In addition, the SMES/battery HESS with the novel droop control can be potentially used in more complicated applications e.g. integrating solar PV, CHP and HESS.

Acknowledgements

All the Authors would like thanks the support by EPSRC EP/K01496X/1, Royal Academy of Engineering, UK.

Table 1

The comparison of the battery only system and hybrid energy storage system.

Cases	Battery			SMES			Total cost (\$)
	Size	Replacement	Cost (\$)	Size	Replacement	Cost (\$)	
Battery only system	28 60 A h	6 times	41,160	N/A	N/A	N/A	41,160
SMES/battery HESS	4 60 A h	4 times	3920	5.27 kJ	0	44,800	48,720

- [42] Li J, Xiong R, Yang Q, Liang F, Zhang M, Yuan W. Design/test of a hybrid energy storage system for primary frequency control using a dynamic droop method in an isolated microgrid power system. Appl Energy 2016. <u>http://dx.doi.org/10.1016/j.apenergy.2016.10.066</u>.
- [43] Mitra P, Venayagamoorthy GK. An adaptive control strategy for DSTATCOM applications in an electric ship power system. IEEE Trans Power Electron. 2010;25:95–104.
- [44] Li J, Zhang M, Zhu J, Yang Q, Zhang Z, Yuan W. Analysis of superconducting magnetic energy storage used in a submarine HVAC cable based offshore wind system. Energy Procedia 2015;75:691–6.
- [45] Fubara TC, Cecelja F, Yang A. Modelling and selection of micro-CHP systems for domestic energy supply: the dimension of network-wide primary energy consumption. Appl Energy 2014;114:327–34.
- [46] Xiong R, He H, Zhao K. Research on an online identification algorithm for a thevenin battery model by an experimental approach. Int J Green Energy 2015;12:272–8.
- [47] Sun F, Xiong R, He H. A systematic state-of-charge estimation framework for multi-cell battery pack in electric vehicles using bias correction technique. Appl Energy 2016;162:1399–409.
- [48] Sun F, Xiong R. A novel dual-scale cell state-of-charge estimation approach for series-connected battery pack used in electric vehicles. J Power Sources 2015;274:582-94.
- [49] Xiong R, Sun F, Gong X, Gao C. A data-driven based adaptive state of charge estimator of lithium-ion polymer battery used in electric vehicles. Appl Energy 2014;113:1421–33.
- [50] Bindner H, Cronin T, Lundsager P, Manwell JF, Abdulwahid U, Baring-Gould I. Lifetime modelling of lead acid batteries. Denmark: Risø Nat. Lab. Roskilde; 2005

- [51] Dufo-López R, Bernal-Agustín JL, Domínguez-Navarro JA. Generation management using batteries in wind farms: economical and technical analysis for Spain. Energy policy 2009;37:126–39.
- [52] Nuhic A, Terzimehic T, Soczka-Guth T, Buchholz M, Dietmayer K. Health diagnosis and remaining useful life prognostics of lithium-ion batteries using data-driven methods. J Power Sources 2013;239:680–8.
- [53] Rychlik I. A new definition of the rainflow cycle counting method. Int J Fatigue 1987;9:119–21.
- [54] Dufo-López R, Bernal-Agustín JL, Yusta-Loyo JM, Domínguez-Navarro JA, Ramírez-Rosado IJ, Lujano J, et al. Multi-objective optimization minimizing cost and life cycle emissions of stand-alone PV-wind-diesel systems with batteries storage. Appl Energy 2011;88:4033-41.
- [55] Moon SH. HTS development and industrialization at SuNAM. 1st Workshop on accelerator magnets in HTS (Hamburg, Germany); 2014.
- [56] Le T, Kim J, Kim D, Boo C, Kim H. Status of the technology development of large scale HTS generators for wind turbine. Progress Supercond Cryogenics 2015;17:18-24.
- [57] Morandi A. HTS de transmission and distribution: concepts, applications and benefits. Supercond Sci Technol 2015;28:123001.
- [58] Grilli F, Kario A. How filaments can reduce AC losses in HTS coated conductors: a review. Supercond Sci Technol 2016;29:083002.
- [59] Wojtasiewicz G, Janowski T, Kozak S, Kondratowicz-Kucewicz B, Kozak J, Surdacki P, et al. HTS magnet for 7.3 kl SMES system. Journal of physics: conference series. IOP Publishing; 2006. p. 821.
- [60] Yuan W, Xian W, Ainslie M, Hong Z, Yan Y, Pei R, et al. Design and test of a superconducting magnetic energy storage (SMES) coil. IEEE Trans Appl Supercond 2010;20:1379–82.